



Contents lists available at ScienceDirect

# Carbohydrate Polymer Technologies and Applications

journal homepage: [www.sciencedirect.com/journal/carbohydrate-polymer-technologies-and-applications](http://www.sciencedirect.com/journal/carbohydrate-polymer-technologies-and-applications)



## Neem-hypericum-bacterial cellulose wound care paste characterized *in vitro* and in *Galleria mellonella in vivo* model

S. Villani<sup>a</sup>, S. Kunjalukkal Padmanabhan<sup>a,\*</sup>, M. Stoppa<sup>a,b</sup>, R. Nisi<sup>b</sup>, M. Calcagnile<sup>c</sup>, P. Alifano<sup>c</sup>, C. Demitri<sup>a</sup>, A. Licciulli<sup>a</sup>

<sup>a</sup> Department of Engineering for Innovation (DII), University of Salento, Lecce, Italy

<sup>b</sup> Biofaber Srl - Brindisi, Italy

<sup>c</sup> Department of Biological and Environmental Sciences and Technologies (DiSTeBA), University of Salento, Lecce, Italy

### ARTICLE INFO

#### Keywords:

Bacterial cellulose  
Neem oil  
Hypericum oil  
Wound healing  
Bacterial biofilm  
*Galleria mellonella*

### ABSTRACT

Surgical wound infections represent a global health emergency because of antibiotic-resistant bacteria. Commensal and pathogenic bacteria can grow in the form of biofilms on damaged skin, and often exhibit an antibiotic-resistance profile. For this reason, the development of new strategies is necessary for the management of skin wounds, which are based not only on antimicrobial activity but also on the inhibition of bacterial biofilm formation or biofilm removal. In this study, we show the development and the biofilm-detaching properties of a novel bacterial cellulose formulation for wound healing. This paste is made by mixing bacterial cellulose pulp with neem-hypericum oil/water emulsion. Once its biocompatibility on murine fibroblasts has been determined, its efficacy was evaluated *in vitro* against *Pseudomonas aeruginosa* and *Staphylococcus aureus* biofilms and *in vivo* by using *Galleria mellonella* larvae as a burn wound infection model. Unlike pure BC, the paste showed promising biofilm detachment properties *in vitro* and a good biocompatibility activity *in vivo*, setting the stage for developing new strategies for the treatment of chronic wound infections.

### 1. Introduction

In the USA and in the European countries, about 2 % of the population is affected by chronic wounds (Falcone et al., 2021). The disruption of the skin integrity enables bacteria to rapidly colonize the injury or the surgical incision (Sen, 2019). Both commensal and pathogen microorganisms can colonize the wound site: they are Gram-positive bacteria, such as *Staphylococcus aureus*, *Enterococcus species*, and Gram-negative bacteria like *Pseudomonas aeruginosa*, *Acinetobacter species*, and fungi like *Candida species* (Sen, 2019). Scientific evidence shows that *S. aureus* usually colonizes the top layer of wounds, while *P. aeruginosa* is localized in the deepest region of the wound bed (Serra et al., 2015). In chronic wounds, *S. aureus* and *P. aeruginosa* react by increasing the expression level of some virulence factors that lead to the development of severe infections and antibiotic resistance (Coates et al., 2014; Vanderwoude et al., 2020). Chronic infections are generally associated with the development of biofilm, a polymicrobial population that adheres to the skin surface and is difficult to eradicate because of the antimicrobial tolerance profile of the microorganisms (Falcone et al.,

2021). Because of the essential role of bacterial biofilm, a major challenge is the development of new strategies that can optimize biofilm eradication in the treatment of chronic wound infection.

Several strategies have been developed to treat wounds, including infection control, dressing selection, topical agents, tissue-based products, and surgical management. Up to now, most of the treatment options for the management of wound infections are based on the application of antimicrobial agents, like iodine and chlorhexidine, or wound dressings. Furthermore, in the case of chronic infections, systemic antibiotics are administered, but this treatment often contributes to the emergence of antibiotic-resistant strains (Kennewell et al., 2019). As a direct consequence of this phenomenon, herbal remedies are gaining more interest as alternative options for the management of chronic infections for the topical treatment of wounds, cuts, and burns. Hypericum oil, obtained from flowering parts of St. John's wort (*Hypericum perforatum L.*), has been used traditionally for the topical treatment of wounds, cuts, and burns due to its occlusive potential on the wound surface as well as its ability to potentiate wound healing by lipophilic phytoactive compounds (hypericin and hyperforin) (Özdemir

\* Corresponding author.

E-mail address: [sanosh.padmanabhan@unisalento.it](mailto:sanosh.padmanabhan@unisalento.it) (S. Kunjalukkal Padmanabhan).

<https://doi.org/10.1016/j.carpta.2024.100431>

Available online 11 January 2024

2666-8939/© 2024 The Author(s). Published by Elsevier Ltd. This is an open access article under the CC BY license (<http://creativecommons.org/licenses/by/4.0/>).

et al., 2023). Among bioactive compounds derived from medicinal plants, neem oil is also reported for the management of chronic wounds: it derives from the plant *Azadirachta indica* and shows antioxidant and anti-inflammatory properties. Neem oil has been already used alone (Banerjee et al., 2021) and in combination with hypericum oil to promote wound healing by increasing the activation of fibroblasts and stimulating collagen synthesis (Özdemir et al., 2023). Carnevali et al. (2006) developed a formulation including neem oil and hypericum oil extracts with healing, repellents, antiseptic, antibacterial, and biocides properties useful for treating external wounds and relieving pain.

Nanocellulose-based composite formulations were developed as carriers for bioactive compounds for wound healing applications (Mef-tahi et al., 2022). Many skin care products with nanocellulose are available in the market owing to their inherent properties like high viscosity and shear thinning, surface functionality, dispersibility, water-holding capacity, purity, and biocompatibility. Cellulose is the most widely available biopolymer in nature, and it is obtained by different methods such as extraction, biosynthesis, enzymatic synthesis, and chemosynthesis (Klemm et al., 2005). Plants and microorganisms are the two main sources of cellulose production. Bacterial cellulose (BC) is the cellulose hydrogel produced by bacteria, like *Komagataeibacter xylinus* (previously known as *Gluconacetobacter xylinus*) (Yamada et al., 2012) by the fermentation of sugar, obtaining cellulose fiber with a high aspect ratio and diameter of less than 100 nm (Klemm et al., 2001). BC has high purity, good water-holding capacity, and biocompatibility compared to vegetable cellulose (VC) derived from wood or cotton. These advantages make them extensively used in various biomedical applications such as drug delivery, tissue engineering, and wound dressing. BC is a good choice for wound healing applications because it can control wound exudate and provide a moist environment for healing. However, using BC alone is not recommended for wound healing as it lacks antibacterial activity (Pal et al., 2017).

Many works report the antibacterial activity of BC hydrogel films (Mef-tahi et al., 2022) incorporated with antibiotics, metal nanoparticles, microbial agents, and natural oils for wound healing applications. In this study, we developed a paste based on fibrillated BC pulp and neem-hypericum oil emulsion. The idea of combining the oil emulsion with the BC pulp arises from the need to optimize the antibacterial properties of BC, together with the search for a valid delivery mode for these natural essential oils.

After biocompatibility tests performed *in vitro* on murine fibroblasts, the safety and the efficacy of the resulting BC/neem-hypericum paste were evaluated *in vivo* by using *Galleria mellonella* larvae as a burn wound infection model (Maslova et al., 2020; Shi et al., 2021). *G. mellonella* is a lepidopteran often used for laboratory studies as a toxicity model for nanotechnology and pharmacological purposes. In this contest, *G. mellonella* larvae can be used as an *in vivo* animal model preliminary to the use of traditional mammalian models, which are more expensive and raise significant ethical restrictions. *G. mellonella*, thanks to its low cost and ease of handling, can contribute to *in vivo* studies as a burn wound infection model, alongside traditional *in vitro* systems, and the more complex *in vivo* mammalian models (Maslova et al., 2020, 2023).

## 2. Materials and methods

### 2.1. BC/neem-hypericum oil paste preparation

Bacterial cellulose (BC) hydrogels were synthesized by Biofaber (Biofaber Srl - Brindisi, Italy) through the fermentation process of the sweetened black tea with *K. xylinus* strains, as reported in our previous work (Pal et al., 2017). Purified BC pellicles were shredded into small pieces and fibrillated using a mini mixer and concentrated at a cellulose content of 2 %. The neem-hypericum oil mix was kindly provided by ENEA (Rome, Italy). For the preparation of the BC-based paste, the pulp was made by concentrating fibrillated BC fragments by centrifugation,

and the aliquot was further concentrated by vacuum pump filtration using a Whatman 41 filter to get cellulose concentration of 7 % wt. Oil-water emulsion of the neem-hypericum with 50 % oil content was prepared using ultrasonic homogenizer (Velp OV5). Pluronic F127 was used as the surfactant and 50 % wt oil in water emulsion was prepared. Finally, the BC/neem-hypericum paste was made by mixing BC pulp and emulsion in a 2:1 ratio and mixed with a homogenizer.

### 2.2. Characterization of BC pulp and neem-hypericum oil/water emulsion

The particle size distribution of BC fibrillated hydrogel was measured by using a CILAS 1190 multi-laser particle size analyzer. The  $\zeta$ -potential of the emulsion was measured using a Malvern zetasizer. The morphology of the BC pulp was analyzed with a Zeiss (Sigma VP, Carl Zeiss, Jena, Germany) Field-Emission Scanning Electron Microscope (FE-SEM). Fourier Transform Infrared Spectroscopy (FTIR) was carried out on Nicolet 6700 spectrometer (Thermo Fisher Scientific Inc., Waltham, MA, USA) in a diffuse reflectance setup accumulating 36 scans over 4000–400  $\text{cm}^{-1}$  wavenumber range. The viscoelastic properties of the wound healing paste were investigated by dynamic mechanical analysis with ARES rheometer from TA instruments (New Castle, DE, USA) with parallel plates. Samples of BC pulp and BC/neem-hypericum paste of 1 mm thickness were tested at 20 °C. To determine the linear viscoelastic regime, dynamic strain sweep measurements at a frequency of 1 Hz with strain ranging between 0.01 % and 100 % were performed. Frequency sweeps between 0.01 and 100 Hz were applied over a linear strain (0.02 %) at 20 °C.

### 2.3. Cell culture and biocompatibility assay

3T3 cell line was maintained in high-glucose Dulbecco's Modified Eagle's Medium (HG-DMEM D5796, Sigma-Aldrich, Milano, Italy), supplemented with 10 % Fetal Bovine Serum (FBS) and penicillin/streptomycin (100 UI/ml), and incubated at 37 °C with 5 %  $\text{CO}_2$  and 99 % humidity. To evaluate the *in vitro* biocompatibility of the BC pulp and the BC/neem hypericum oil paste, a direct contact test was performed.

Cell proliferation assay was performed by using 3-[4,5-dimethylthiazol-2-yl]-2,5 diphenyl tetrazolium bromide (MTT) test after 24 h of direct contact between fibroblasts and the formulations investigated. MTT is a colorimetric method used to assess the cellular viability through the metabolic activity of viable cells in converting the yellow tetrazolium salt into an insoluble purple formazan precipitate. By spectrophotometric analysis, it was possible to quantitatively assess the intensity of the staining, which is related to the amount and vitality of cells. To evaluate their biocompatibility, two solutions of 10 % and 1 % w/v were prepared by dispersing BC pulp and BC paste in the complete culture medium. 3T3 cells were seeded at a density of  $1.0 \times 10^5$  cells/ml in a 96-well plate in HG-DMEM medium. After 24 h of incubation, the culture medium was replaced with 200  $\mu\text{l}$  of 10 % or 1 % solutions of BC pulp and BC paste, whereas control cells (CTRL) were incubated with fresh medium. After 24 h of incubation, the culture medium was removed, and the proliferation assay was performed. A 5 mg/ml solution of MTT in Phosphate Buffered Saline (PBS) was further 1:10 diluted in complete culture medium and 200  $\mu\text{l}$  were added to each well. After 3 h of incubation at 37 °C, formazan crystals formed in the cells were dissolved in 200  $\mu\text{l}$ /well of acidified isopropanol (37 % HCl in isopropanol). The absorbance was measured at 550 nm by using a spectrophotometer. The viability of fibroblast cells is shown as percentage of absorbance relative to untreated CTRL cells.

### 2.4. Biofilm detaching properties evaluation

*P. aeruginosa* GG-7 (Calcagnile et al., 2023; Tredici et al., 2018) and *S. aureus* SA-1 (Calcagnile et al., 2022) were grown in Luria-Bertani (LB) broth with shaking at 120 rpm at 37 °C. The composition of the LB medium (per liter) was: 10 g of NaCl, 10 g of Tryptone, 5 g of Yeast

Extract. LB Agar was supplemented with 15 g of Agar per liter. The bacterial pre-inoculum was prepared by making a suspension in liquid LB medium of an isolated colony selected from a fresh agar plate, and then incubated overnight (ON) at 37 °C. The day after, bacteria were resuspended in the medium reaching an Optical Density (OD) of 0.3–0.4 at 600 nm and further 1:50 diluted. Then, each of the 12-well plates containing 15 mm square coverslips was inoculated with 2 ml of *P. aeruginosa* or *S. aureus* suspension and incubated at 37 °C for 24 h.

Two solutions of 10 % and 1 % w/v of paste were prepared in NaCl 0.9 %. After 24 h of biofilm growth, coverslips were treated with 2 ml of 10 % or 1 % paste solution for 5 min. Some samples were treated for 5 min with 2 ml of NaCl 0.9 % as a control and with 2 ml of 1 % Sodium Dodecyl Sulfate (SDS) as a standard cleaning agent (Diaz De Rienzo et al., 2016). To better investigate BC paste detachment properties, 10 % and 1 % solutions of VC and fibrillated BC pulp were prepared in NaCl 0.9 %, to be used as a comparative agent. To determine the number of Colony Forming Unit (CFU/ml), the different types of coverslip samples were put in 2 ml of LB medium and vortexed for 2 min. Then, 10 µl of the liquid phase was diluted and spotted on solid LB Petri dishes and incubated at 37 °C until the next day. Each coverslip sample was also fixed and subjected to crystal violet staining to carry out a microscopy analysis using Leica LB30S light microscope (Leica Microsystems Wetzlar GmbH).

Together with the *in vitro* analysis of the biofilm detaching activity, a microscopy analysis was carried out to study the affinity between bacterial cells and BC fibers. *P. aeruginosa* and *S. aureus* pre-inocula were prepared as described above, and incubated ON at 37 °C. The next day, the bacterial pre-inocula were adjusted until an OD of 0.3–0.4 at 600 nm. Then, they were 1:50 diluted in a 10 % solution of BC/neem-hypericum oil paste and incubated ON at 37 °C. At the end of the incubation period, the samples were processed differently according to the microscopy technique to be used. To conduct light microscopy analysis, the bacterial cell suspension was fixed, stained with crystal violet, and observed under microscope (Leica Microsystems Wetzlar GmbH). In the case of SEM investigations, bacterial samples were fixed by air-dehydration in a fume hood for 40 min and were stored at 4 °C before examination.

## 2.5. Establishment of the burn wound infection model with *G. mellonella* larvae

*G. mellonella* larvae were purchased from a local fishing supply store and stored at room temperature before being used. To set up the experimental design, 5 adult *G. mellonella* larvae per group were chosen, with an average weight within the range (250 ± 50) mg. Before starting, larvae were left without feeding for 3 days to exclude any variability due to larval feeding and defecation before the experiment and during the observation period. A disinfection protocol for the larval dermis was adopted before being used for the experiment, to remove bacteria colonizing the larval skin. As reported in literature (Maslova et al., 2023; Shi et al., 2021), the larval body was sterilized with 70 % ethanol, and the treated larvae were sorted in sterile Petri dishes to preserve their sterility. The burn was realized following a protocol described in literature (Shi et al., 2021). More in detail, a metal spatula was heated and applied in the middle section of the larval back for 4 s, realizing a burn area of approximately 2 mm<sup>2</sup>. Any larvae that showed hemolymph loss or protruding fat body after the procedure was euthanized by placing it at -20 °C. For the infection experiment, after 20 min post burn, the wound was inoculated with 10 µl of 1:10 dilution of a bacterial ON culture (equivalent to an OD of 0.200 at 600 nm). After 1 h, *G. mellonella* larvae were treated with BC/neem-hypericum oil paste, applying a quantity sufficient to cover the wound site (~ 100 mg), or with 200 µl of 10 % solution of BC paste as a cleaning solution. The BC-based formulations were also applied on intact skin and on the uninfected burn site to evaluate the safety and toxicity *in vivo*. *G. mellonella* larvae were incubated at 37 °C and mortality was evaluated during the following days, observing a complete melanization of the body and a complete loss

of motility. The experiment has been conducted in duplicate.

## 2.6. Statistical analysis

The data are presented as the Mean ± Standard Deviation (SD) for the indicated number of experiments. The statistical analysis was conducted by using One Way ANOVA, followed by Tuckey's test for multiple comparisons with respect to the control (CTRL). In all comparisons,  $p < 0.05$  was considered statistically significant, and the significance level was reported when present.

## 3. Results

### 3.1. BC and BC/neem-hypericum paste characterization

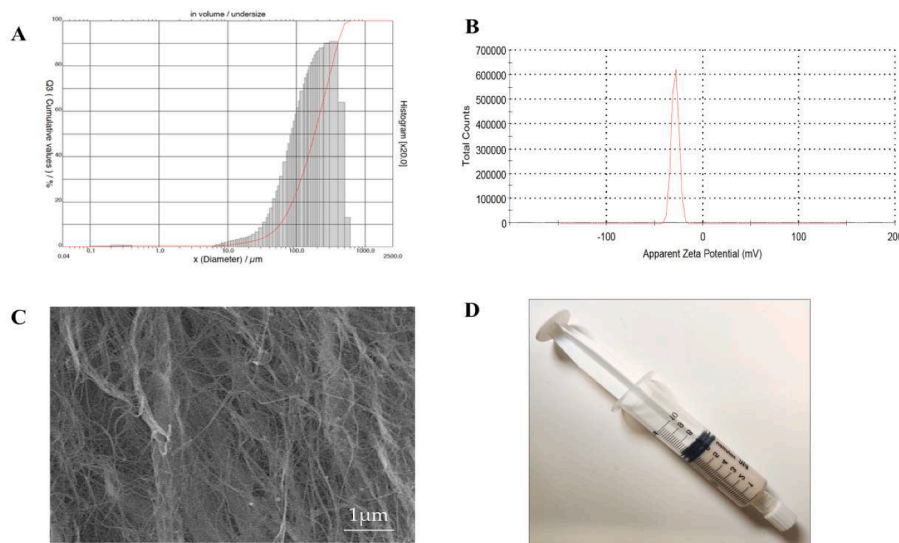
Fig. 1A shows the particle size distribution of fibrillated BC: an average particle size of 200 µm was attained after fibrillation, showing that the mini mixer process succeeded in obtaining BC pulp without any lumps. ζ-potential of the emulsion was measured, and -29 mV was observed for neem-hypericum/water emulsion indicating the stability of the emulsion (Fig. 1B). The microstructure observed by SEM in Fig. 1c showed that even after fibrillation, cellulose retained the nanofibrous structure after fibrillation without destroying the 3-D network. Finally, after proper mixing with BC pulp and oil emulsion, an injectable paste was obtained (Fig. 1D).

Fig. 2 shows the FT-IR spectra of fibrillated BC, neem-hypericum oil and BC/neem-hypericum paste. Typical stretching and vibrational bands of cellulose I appeared for fibrillated BC; spectrum at 3405 cm<sup>-1</sup> for O-H stretching, 1647 cm<sup>-1</sup> for H-O-H bending vibration of absorbed water molecules; 1427 cm<sup>-1</sup> for CH<sub>2</sub> symmetrical bending, 1164 cm<sup>-1</sup> for C—O—C bond and 1110 cm<sup>-1</sup> for C—O stretching for b-linked glucose polymers (Padmanabhan et al., 2022; Pal et al., 2017).

Peaks associated with C-H stretching band specific to *H. perforatum* oil and neem oil were observed at 2854 and 2923 cm<sup>-1</sup>; this showed the presence of aliphatic C—H stretch present in the oil. The C=O stretch of the triglyceride ester of the oil appeared at 1749 cm<sup>-1</sup>, and for C—H bending at 1467 cm<sup>-1</sup>. The presence C—O—C stretching vibration of the esters was inferred at peaks 1166 cm<sup>-1</sup> and methylene rocking vibration present in the oil was evident at peak 719–723 cm<sup>-1</sup>. Peaks correspond to cellulose and neem/hypericum oil was evident in BC/oil paste. The results obtained from FT-IR-ATR analysis revealed that neem-hypericum oil mix was successfully loaded to the BC pulp and that the compounds integrated with BC resulted in no changes in the chemical structure.

The shear rate dependence of the steady viscosity for BC pulp and BC/neem-hypericum paste at 20 °C is shown in Fig. 3A. It is observed that the apparent viscosity of BC/neem-hypericum paste is more than two orders of magnitude higher than that of BC pulp. For example, at a shear rate of 0.1 s<sup>-1</sup>, the apparent viscosity of BC/neem-hypericum paste is more than 500 Pa\*s, whereas that of BC pulp is less than 1 Pa\*s. The samples exhibit a classical thixotropic behavior within the investigated share rate range (0.1–100 s<sup>-1</sup>). This phenomenon could be attributed to the hydrodynamic forces generated by the shear rates that cause BC aggregates to become deformed and eventually disrupted, resulting in a reduction in the viscosity. The control sample (without oil) showed a lower viscosity; while, in the case of BC/neem-hypericum oil mix, a higher viscosity was observed. This result can be ascribed to the large contact surface area between oil droplets and the continuous phase that opposes the free flow of the emulsion. The oil droplets are close enough to interact with each other, thus leading to an increase in the viscosity of the system (Zhang et al., 2020). This behavior helps the investigated paste to remain on the wound site without flowing.

The viscoelastic behavior is presented in Fig. 3B where there is a head-to-head comparison between the storage modulus ( $G'$ ) and loss modulus ( $G''$ ) of BC pulp and BC/neem-hypericum paste. In BC/neem-hypericum paste is evident that there is a frequency in which a phase separation occurs. A crossover point is reached at around 10 rad/sec.



**Fig. 1.** (A) Particle size distribution of fibrillated BC. (B)  $\zeta$ -potential measurement of neem-hypericum oil/water emulsion. (C) SEM image of fibrillated BC. (D) Photograph of injectable BC/neem-hypericum paste.

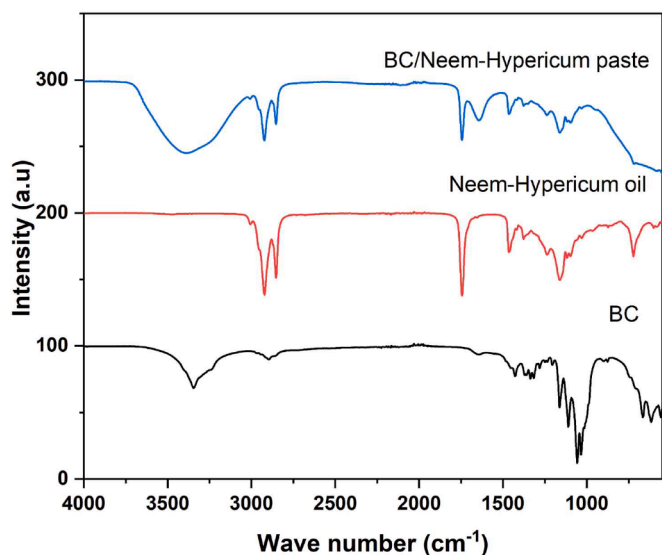


**Fig. 2.** FT-IR spectra of fibrillated BC, neem-hypericum oil emulsion and BC/neem-hypericum paste.

Below this point, both pastes are stable and react as a suspension showing higher  $G'$  than  $G''$ . At higher frequencies, the viscoelastic properties change due to a possible phase separation between the solid and liquid components. In the case of BC paste the water is released out from the fibril matrix, while in the case of BC/neem-hypericum paste the structure seems to be more stable even though a crossover point could be detected. These differences can be attributed to the presence of stable emulsion if compared to the BC sample in which only water is present.

### 3.2. Biocompatibility evaluation *in vitro*

The 3T3 fibroblast cell line was chosen to evaluate the *in vitro* biocompatibility of BC pulp and BC-based paste. For this purpose, the direct contact method with 10 % and 1 % solutions of BC pulp and paste was adopted, evaluating cell viability *via* MTT assay after 24 h. From this *in vitro* model, cell viability emerged comparable to the control after 24 h of contact with the investigated materials, without observing statistically significant differences. Fig. 4 shows the cell viability normalized to the CTRL. As reported in the International Standard ISO 10993-5:2009 “Biological evaluation of medical devices - Tests for *in vitro* cytotoxicity” (ISO 10993-5:2009), a 30 % reduction in the cell viability can be attributed to the cytotoxicity of the investigated material. For this reason, in Fig. 4 the cell viability value corresponding to 70

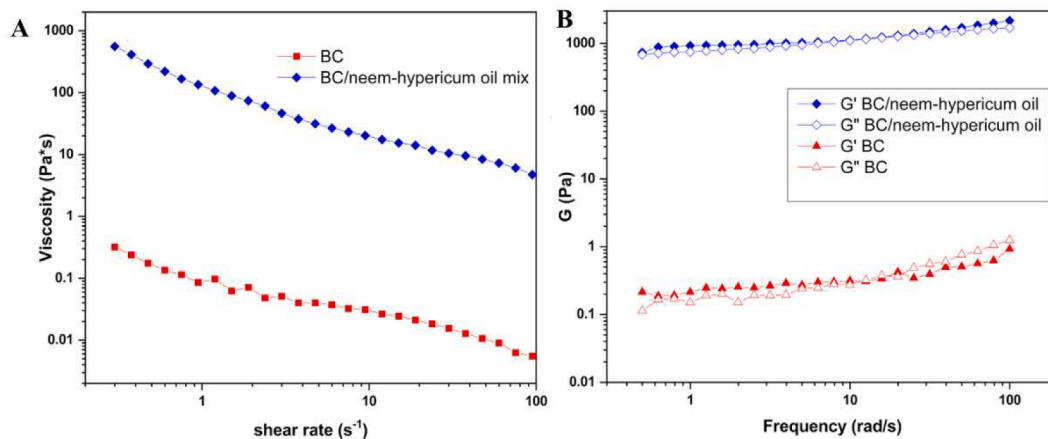


**Fig. 3.** Rheological features of BC and BC/neem-hypericum paste: (A) dynamic strain sweep and (B) frequency sweep test.



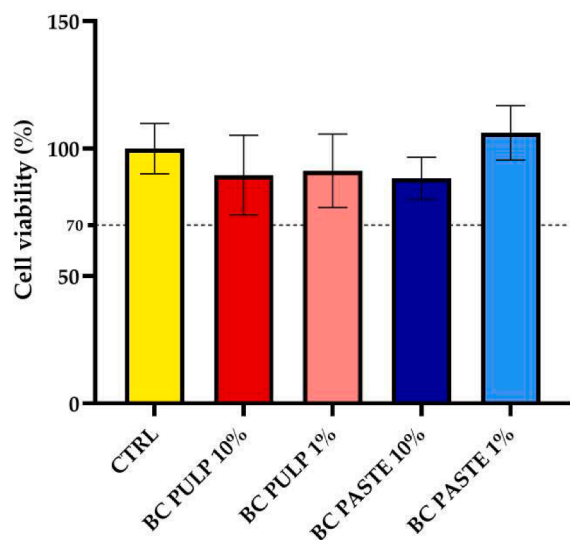


**Fig. 4.** 3T3 fibroblasts viability, expressed as a percentage calculated compared to the control (CTRL), after direct contact with the 10 % and 1 % solutions of BC pulp and BC paste for 24 h.

% is highlighted as the threshold necessary to exclude the cytotoxicity of the investigated formulations.

### 3.3. Biofilm detaching properties evaluation

*P. aeruginosa* and *S. aureus* were chosen to test the biofilm removal properties of the BC/neem-hypericum oil paste, as these two bacteria often colonize the surface of chronic wounds and are commonly involved in wound infections. The protocol was based on the ability of several bacteria to form biofilm on coverslips and was standardized for both species, leading to the formation of a 24 h bacterial biofilm that

could be used for biofilm detachment tests. To estimate the capability of the paste to eradicate bacterial biofilms, the quantification of CFU/ml was chosen, and these results were confirmed by light microscopy analysis. To conduct the biofilm detachment test, a contact period of 5 min between the biofilm and the detachment agent was chosen as application time for a cleansing agent to be used for skin lesions.

In this *in vitro* model, the BC/neem-hypericum paste showed promising biofilm eradication properties for both bacterial species investigated. In particular, the application of 10 % solution of BC/neem-hypericum paste reduced the number of CFU/ml of *P. aeruginosa* (Fig. 5A) and *S. aureus* (Fig. 5B). In both cases, the use of a 10 % paste solution showed better biofilm detachment properties than SDS, which is considered a common cleaning agent capable of destroying bacterial biofilm (Ashori et al., 2014; Castro et al., 2011). Also, the application of a 1 % solution of BC/neem-hypericum paste showed remarkable biofilm detachment properties which were more evident for *S. aureus* than for *P. aeruginosa* biofilm (Fig. 5B). The use of 1 % and 10 % VC solutions also showed stronger detachment capabilities against *S. aureus* biofilm than *P. aeruginosa* biofilm; however, VC detachment properties appeared to be inferior than those of BC/neem-hypericum paste for both bacterial species. This investigation continued by conducting a light microscopy analysis to support the quantitative evaluation of the CFU/ml assay. A 5-min treatment with the 10 % solution of BC/neem-hypericum paste resulted in a marked reduction in the biofilm density for both *P. aeruginosa* (Fig. 5C) and *S. aureus* (Fig. 5D) compared to the control. The performance obtained with the 10 % solution of BC/neem-hypericum paste was also better than that of the VC solutions and of the 1 % SDS (Fig. 5).

To explain the biofilm removal mechanism by which the BC paste detached the *P. aeruginosa* and *S. aureus* biofilms, an affinity between bacterial cells and BC fibers was hypothesized. The ability of the BC fibers to bind bacterial cells was analyzed to confirm this hypothesis. As reported in Fig. 6, both *P. aeruginosa* and *S. aureus* cells showed significant adhesion on BC fibers after 24 h of incubation, with an interesting tendency to locate along the polymeric fiber, as seen in light microscopy

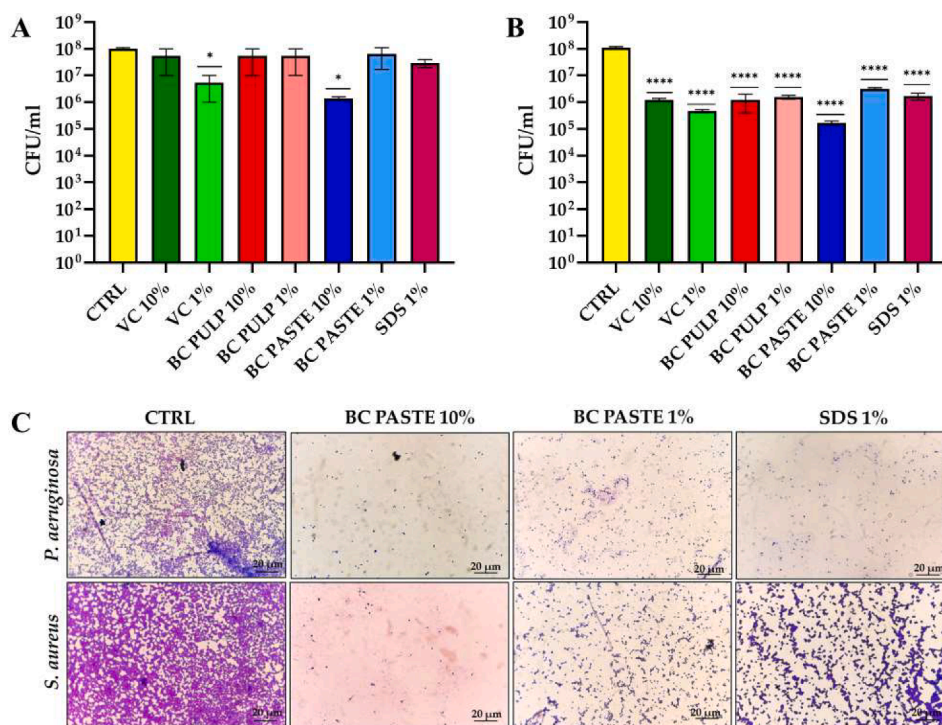


**Fig. 5.** Determination of CFU/ml of (A) *P. aeruginosa* and (B) *S. aureus* biofilms after 5 min treatment with 10 % or 1 % vegetal cellulose solution, 10 % or 1 % BC pulp solution, 10 % or 1 % BC paste solution, or 1 % SDS as a standard cleaning agent. (C) Light microscopy analysis of the resulting biofilms after the treatment. \*  $p < 0.05$ ; \*\*  $p < 0.01$ ; \*\*\*  $p < 0.001$ ; \*\*\*\*  $p < 0.0001$ .

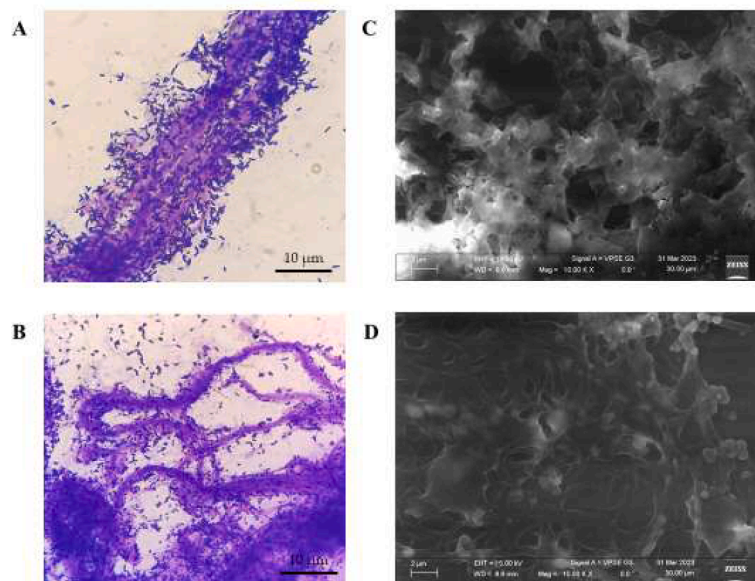


**Fig. 6.** Light microscopy and FE-SEM images of (A,C) *P. aeruginosa* and (B,D) *S. aureus* cells attached on BC fibers in BC/neem-hypericum paste after 24 h of incubation.

and SEM images.

### 3.4. Evaluation of the biocompatibility and efficacy in the *G. mellonella* model of infected burn

To validate the biocompatibility and the efficacy of BC/neem-hypericum paste, *G. mellonella* larvae were used as an alternative to the traditional mammalian models. The experiment has been conducted in duplicate, reporting results by using the Kaplan–Meier survival curve (Fig. 7B,C,D). Data obtained, reported as Mean  $\pm$  Standard Deviation of the survival percentage obtained from the number of replicates indicated above, are reported in Supplementary Material (Table 1 and Fig. 1). As shown in Fig. 7, BC/neem-hypericum formulation proved to

be completely biocompatible in case of intact skin if applied both as a paste and as a cleansing solution. In the case of non-infected injured skin, the application of the biomaterials made it possible to increase the survival rate from 30 % to 80 % by applying the paste, and to 60 % by using the 10 % detergent solution after 24 h of treatment. In the case of infected burn wounds, the application of the BC-based paste ensured a 30 % survival (compared to 100 % mortality in untreated larvae) of the animals infected with *P. aeruginosa* one day after treatment, and 70 % (compared to a survival of 20 % in untreated animals) of the animals infected with *S. aureus* infection two days after treatment.

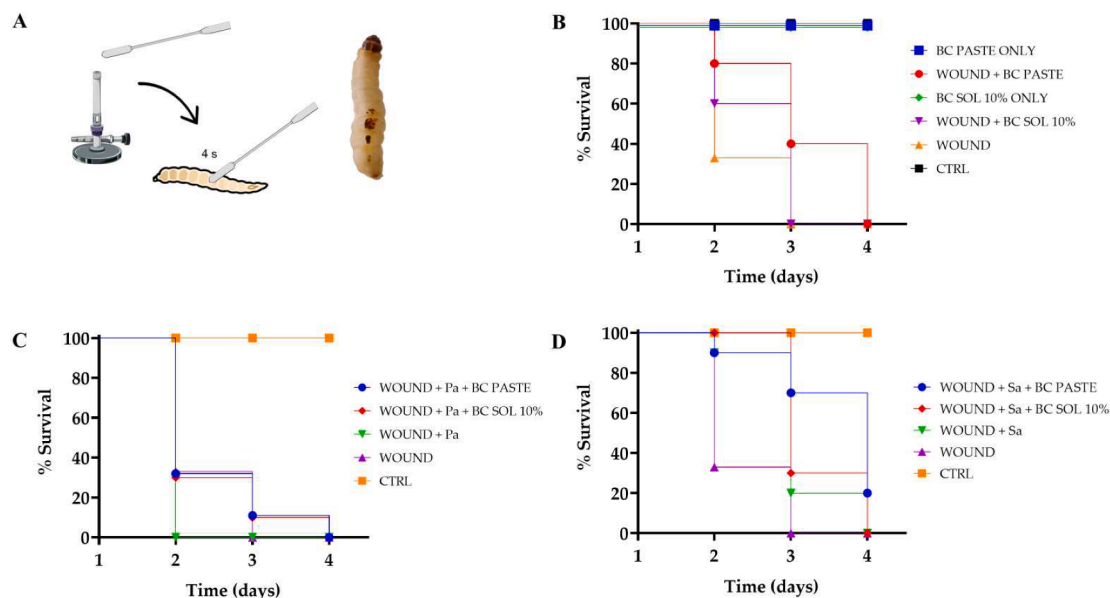


**Fig. 7.** Evaluation of the efficacy and biocompatibility of BC/neem-hypericum formulation applied as a paste or as a 10 % cleaning solution by evaluating the survival rate of *G. mellonella* larvae. On the top, (A) a schematic representation of the protocol used to realize the burn and (B) an evaluation of the safety of the formulations on intact skin and uninfected burn wounds. On the bottom, an evaluation of the efficacy of the treatment of burn wounds infected by (C) *P. aeruginosa* (Pa) and (D) by *S. aureus* (Sa).

#### 4. Discussion

The emergence of antibiotic-resistant microorganisms has necessitated the development of new antibacterial strategies for the treatment of bacterial infections. Surgical wound infections are a serious health problem as they hinder the normal healing process of the injured skin. In the perspective of circular economy, the production of cellulose hydrogels through a bacterial fermentation process can represent an excellent opportunity for the recovery of waste material (Padmanabhan et al., 2022; Srivastava et al., 2023). In this study, BC nanofibers were added to a mixture of neem and hypericum oils for the development of a novel strategy of wound management with antibacterial properties. By proper fibrillation of bacterial cellulose and mixing with neem-hypericum oil emulsion, we could successfully prepare a paste having water holding capacity of cellulose nanofibers and antibacterial properties of neem-hypericum oil. A moisturizing environment is essential for the damaged skin to promote the wound healing process. The BC component in our paste can provide temporary and prompt wound coverage and a mechanical barrier to infections and in the meantime, it can absorb the wound exudate, thus keeping a moist environment to facilitate debridement of the necrotic tissue and spontaneous re-epithelialization of the skin. Thanks to this antibiotic-free approach in favour of the neem-hypericum oil formulation, this paste can further protect the wound bed from undesired microbial contaminations (Winter, 1962).

The resulting formulation was investigated *in vitro* by evaluating its biofilm-detaching activity against *P. aeruginosa* and *S. aureus* biofilms. For this purpose, 1 % and 10 % solutions of BC-based paste were prepared and applied as a detergent solution on bacterial biofilms for 5 min, as a plausible application time for a cleansing agent to be used for skin lesions; further investigations are needed to better investigate the time-response behavior of the formulation in the detachment of bacterial biofilms. This study showed that BC-based paste has interesting detaching properties of bacterial biofilms produced by *P. aeruginosa* and *S. aureus*, appreciable in the reduction of the CFU/ml adherent on the coverslip compared with the untreated sample. Fibrillated BC pulp alone was ineffective in the biofilm-detaching activity, supporting the synergistic effect if combined with neem-hypericum oil.

As described previously, BC has better biocompatibility and higher water-holding capacity than VC (Pal et al., 2017). Since BC has been shown to be more suitable in wound dressing than the vegetal counterpart (Pal et al., 2017), 10 % and 1 % VC solutions were adopted for comparison, proving to be less effective than BC-based solutions. The bacterial affinity for BC fibers has been confirmed by light microscopy and FE-SEM investigations, showing an interesting tendency of bacterial cells to adhere to the BC fibers in the formulation. Up to now, most of the biofilm eradication strategies are based on the addition of antibacterial agents, like antimicrobial peptides and lipids, or antibiotics (Verderosa et al., 2019). Alternatively, polymeric materials like hydrogels and nanocomposites with cationic or charge-switchable macromolecules are exploited for their biofilm-detaching ability (Banerjee et al., 2021). On the contrary, it is possible to exploit the recognition between bacterial cells and cellulose fibers to exert a biofilm-removal activity on bacterial biofilms. Scientific evidence shows that glycosaminoglycans (GAGs) are strongly involved in the bacterial adhesion process to eukaryotic cells. Some microbial pathogens exploit the presence of some specific adhesins that mediate the GAGs bounds (Rajan et al., 2020; Rajas et al., 2017). As a result, a recent study developed a cellulose-based nanomaterial with antibiofilm activity that was structurally inspired by GAGs to mimic their action during the bacterial adhesion process (D'Orazio et al., 2017). The same phenomenon could describe the biofilm-detaching efficacy observed for the BC-based paste, promoting its use for the management of chronic wound infections. The greater effectiveness of BC-based materials when compared with VC in the detachment activity can be explained by the different source of isolation that could have repercussions on the cell-fiber recognition and, therefore, on the

biofilm-detaching activity itself. In combination with BC fibers, the neem/hypericum oil emulsion could contribute to the antibiofilm activity of the resulting formulation. As described in several scientific works, neem oil is a source of various compounds effective against bacterial biofilms: the limonoid nimbolide is effective against methicillin-resistant *S. aureus* (MRSA) (Sarkar et al., 2016), and the phenol catechin acts as an antibiofilm agent against dental biofilm (Lahiri et al., 2021). In addition, *H. perforatum* proved itself to have antibiofilm effects: hypericum oil has been used against common pathogens responsible for periodontitis (Bagheri et al., 2022), and *H. perforatum* extracts have been characterized to promote their use as antibiofilm agents in oral care products (Süntar et al., 2016). The different efficacy observed between *P. aeruginosa* and *S. aureus* can be attributed to a different architecture of the biofilm, together with a different cellular morphology and structure, and a different cell wall (Schilcher & Horswill, 2020; Thi et al., 2020). Further investigations will be conducted to study the behaviors of other types of cellulose, and additional bacteria species will be tested, even in a polymicrobial film.

Currently, the in-depth study of the burn wound microenvironment is hampered by the need to involve *in vivo* mammalian models such as mice, rats, and pigs, which raises ethical questions. For this reason, the promotion of an invertebrate model is fundamental from an ethical point of view, together with the possibility of making notable improvements in the study of tissue regeneration mechanisms and in the development of effective clinical treatments. A recent study demonstrated that *G. mellonella* model could mimic the hallmark of burn trauma seen in patients, such as decreased survival prognosis with increased burn surface area and the importance of rapid fluid resuscitation, together with the possibility to study the biofilm formation at the burn wound site (Maslova et al., 2020).

To verify the biocompatibility of the formulation obtained by mixing BC with neem and hypericum oils, the 3T3 cell line of murine fibroblasts was adopted for preliminary *in vitro* studies. This study aimed to exclude the cytotoxicity of the formulation placed in direct contact with fibroblasts. In particular, the impact of the materials on cell viability was quantified spectrophotometrically by MTT assay, exposing cells to a 10 % or 1 % solution of BC pulp or paste. The International Standard ISO 10993-5:2009 “Biological evaluation of medical devices - Tests for *in vitro* cytotoxicity” (ISO 10993-5:2009), which regulates the evaluation of the biocompatibility of medical devices *in vitro*, establishes that a reduction in cell viability greater than 30 % is to be considered the result of a cytotoxic effect of the material investigated. The test conducted on murine fibroblasts placed in contact with the investigated materials revealed a cellular viability comparable to that of untreated cells, without significant differences between the BC pulp and the BC-based paste. Furthermore, no significant differences in cell viability were observed as the concentration of the tested solutions increased. This allowed to certify the *in vitro* biocompatibility of the BC/neem formulation.

In this study, *G. mellonella* made it possible to have a preliminary assessment of the safety and efficacy of the materials being studied in line with the 3Rs principles (Replace, Reduce, Refine) and without the involvement of mammalian models (Mannala, 2020). Together with the lower costs, the availability of the animals, and the absence of ethical limitations, the *G. mellonella* model is more advantageous than many other animal models also due to the faster execution of the tests and easier interpretation of the results, thanks to the possibility of following two markers of viability: the melanization process and the larval motility (Djokaite et al., 2021; Scorzoni et al., 2013). Despite the frequent use of *G. mellonella* as a model *in vivo* of toxicity and infection, only few studies exploited *G. mellonella* as a model of infected burn wounds to be treated through the application of biomaterials for wound management (Maslova et al., 2023; Shi et al., 2021). In this study, *G. mellonella* has proven to be a useful tool for creating infected burn lesions *in vivo*, and the *in vivo* results support the observed efficacy of BC/neem-hypericum paste. In the case of non-infected skin lesions, the



application of the BC-based formulations made it possible to increase the survival rate from 30 % to 80 % by applying the paste, and to 60 % by using the 10 % detergent solution. In the case of infected burn wounds, the survival rate increased to 40 % by applying both paste or cleaning solution against *P. aeruginosa* infected burn wounds after 24 h, and from 20 % to 50 % after 48 h in the case of *S. aureus* infected wounds. The increase in the survival rate of *G. mellonella* could be due to the ability of the paste to create a microenvironment suitable for the wound healing, together with the capability to attract the bacterial cells, as supported by the *in vitro* experiments. This phenomenon would lower the bacterial load at the site of the burn wound and promote the regeneration of the injured tissue that may be also favored by a more humid microenvironment and better management of wound exudates (Cullen & Gefen, 2023).

Although *G. mellonella* has been a useful tool in validating treatment effectiveness *in vivo*, there are some limitations to consider when using it as an animal model. The larvae are commonly purchased from fishing shops, and a standardized diet is missing: these aspects can affect the reproducibility of the experiments, impacting the larval health and ultimately the experiment's outcome. Additionally, creating a skin lesion on the larvae's back is a crucial step that requires careful attention, as the larval cuticle is thin and close to its internal systems (Maslova et al., 2023). This step, coupled with the possible movements of the larvae during the procedure, could affect the reproducibility and accuracy of the method. Progress in standardizing protocols for using larvae could contribute significantly to enhancing research in the field of nanotechnology and materials and promote the use of alternative *in vivo* models. While *G. mellonella* can't fully replace traditional mammalian models today, it still presents itself as a valuable tool for validating treatment efficacy *in vivo* as a burn wound model.

## 5. Conclusion

This work highlights the synergistic effect of BC and neem-hypericum oil emulsion (naturally derived antibacterial agents) in creating a paste for wound healing application. The cytotoxicity was previously excluded by *in vitro* biocompatibility tests on murine fibroblasts, and the biofilm-detaching activity was first evidenced *in vitro* against *P. aeruginosa* and *S. aureus* biofilms. Even more interestingly, the effectiveness of the medical treatment containing bacterial cellulose was tested for the first time with the *G. mellonella* larvae method. Although the involvement of *G. mellonella* needs improvement to ensure the reproducibility and scientific rigor of the experiments, it has proven to be a useful tool for realizing infected burn lesions *in vivo* tests. This method was effective in evaluating the advantages of bacterial cellulose over vegetable cellulose and emulsion alone. The *in vivo* method used to preliminarily assess the biocompatibility and the efficacy of the BC-based paste could represent a crucial promotion opportunity of the use of *G. mellonella* larvae as a burn wound infection model. This feature will be further investigated in the future, in combination with the regenerative effect of BC.

This result, suitably supported by further investigations, could pave the way for the development of a new formulation to be applied as a paste, patch or as a cleansing solution for the removal of colonizing microorganisms from damaged skin.

## Funding

This work was supported by the Italian Minister of Research with the Ministerial Decree n. 351/2022 — PNRR Mission 4, Component 1 and Regione Puglia for funding REFIN—Research for Innovation project “Medicazioni innovative per rigenerazione tissutale a base di idrogeli funzionalizzati di cellulosa batterica”, project no. 8AE55352, in the framework of POR PUGLIA FESR-FSE 2014/2020 projects.

## CRedit authorship contribution statement

**S. Villani:** Investigation, Methodology, Writing – original draft, Visualization. **S. Kunjalukkal Padmanabhan:** Investigation, Methodology, Writing – original draft, Visualization. **M. Stoppa:** Investigation, Methodology. **R. Nisi:** Investigation, Methodology. **M. Calcagnile:** Investigation, Methodology, Writing – review & editing. **P. Alifano:** Conceptualization, Writing – review & editing, Supervision. **C. Demitri:** Conceptualization, Writing – review & editing, Supervision. **A. Licciulli:** Conceptualization, Writing – review & editing, Supervision.

## Declaration of competing interest

The authors declare that they have no known competing financial interests or personal relationships that could have appeared to influence the work reported in this paper.

## Data availability

Data will be made available on request.

## Acknowledgements

Sanosh Kunjalukkal Padmanabhan acknowledges Regione Puglia for funding REFIN—Research for Innovation project “Medicazioni innovative per rigenerazione tissutale a base di idrogeli funzionalizzati di cellulosa batterica”, project no. 8AE55352, in the framework of POR PUGLIA FESR-FSE 2014/2020 projects.

The authors thank Dr. Fiorella Carnevali (ENEA Rome, Italy) for providing neem-hypericum oil mix.

The icons used for graphical abstract realization were downloaded from bioicons.com: fly larva icon by DBCLS <https://togovt.dbcls.jp/en/pics.html> is licensed under CC-BY 4.0 Unported <https://creativecommons.org/licenses/by/4.0/>, modified in the color; spatula-top icon by OpenClipart <https://openclipart.org/> is licensed under CC0 <https://creativecommons.org/publicdomain/zero/1.0/>; micropipette icon by Servier <https://smart.servier.com/> is licensed under CC-BY 3.0 Unported <https://creativecommons.org/licenses/by/3.0/>; bunsen-burner icon by Servier <https://smart.servier.com/> is licensed under CC-BY 3.0 Unported <https://creativecommons.org/licenses/by/3.0/>; ointment icon by Servier <https://smart.servier.com/> is licensed under CC-BY 3.0 Unported <https://creativecommons.org/licenses/by/3.0/>. Last access: 31 July 2023.

This study has been carried out using the facilities of the Biodiversity Organization and Ecosystem Functioning (BIOforU)-node1.

## Supplementary materials

Supplementary material associated with this article can be found, in the online version, at [doi:10.1016/j.carpta.2024.100431](https://doi.org/10.1016/j.carpta.2024.100431).

## References

- Ashori, A., Babae, M., Jonoobi, M., & Hamzeh, Y. (2014). Solvent-free acetylation of cellulose nanofibers for improving compatibility and dispersion. *Carbohydrate Polymers*, 102, 369–375. <https://doi.org/10.1016/j.carbpol.2013.11.067>.
- Bagheri, R., Bohloui, S., Maleki Dizaj, S., Shahi, S., Memar, M. Y., & Salatin, S. (2022). The Antimicrobial and anti-biofilm effects of hypericum perforatum oil on common pathogens of periodontitis: an *in vitro* study. *Clinics and Practice*, 12(6), 1009–1019. <https://doi.org/10.3390/clinpract12060104>
- Banerjee, K., Chatterjee, M., Sandur V, R., Nachimuthu, R., Madhyastha, H., & Thiagarajan, P. (2021). Azadirachta indica A. Juss (Neem) oil topical formulation with liquid crystals encompassing depot water for anti-inflammatory, wound healing and anti-methicillin resistant Staphylococcus aureus activities. *Journal of Drug Delivery Science and Technology*, 64, Article 102563. <https://doi.org/10.1016/j.jddst.2021.102563>



- Calcagnile, M., Jeguirim, I., Tredici, S. M., Damiano, F., & Alifano, P. (2023). Spiramycin disarms *Pseudomonas aeruginosa* without inhibiting growth. *Antibiotics*, 12(3), 499. <https://doi.org/10.3390/antibiotics12030499>
- Calcagnile, M., Tredici, M. S., Pennetta, A., Resta, S. C., Talà, A., De Benedetto, G. E., & Alifano, P. (2022). *Bacillus velezensis* MT9 and *Pseudomonas chlororaphis* MT5 as biocontrol agents against citrus sooty mold and associated insect pests. *Biological Control*, 176, Article 105091. <https://doi.org/10.1016/j.biocontrol.2022.105091>
- Carnevali, F., & Van Der Esch, S. A. (2006). *Composition comprising neem oil and oil extract of hypericum having healing, Repellent and Biocidal Properties for Treating External Wounds*.
- Castro, C., Zuluaga, R., Putaux, J.-L., Caro, G., Mondragon, I., & Gañán, P. (2011). Structural characterization of bacterial cellulose produced by *Gluconacetobacter swingsii* sp. From Colombian agroindustrial wastes. *Carbohydrate Polymers*, 84(1), 96–102. <https://doi.org/10.1016/j.carbpol.2010.10.072>
- Coates, R., Moran, J., & Horsburgh, M. J. (2014). Staphylococci: Colonizers and pathogens of human skin. *Future Microbiology*, 9(1), 75–91. <https://doi.org/10.2217/fmb.13.145>
- Cullen, B., & Gefen, A. (2023). The biological and physiological impact of the performance of wound dressings. *International Wound Journal*, 20(4), 1292–1303. <https://doi.org/10.1111/iwj.13960>
- Díaz De Rienzo, M. A., Stevenson, P. S., Marchant, R., & Banat, I. M. (2016). *Pseudomonas aeruginosa* biofilm disruption using microbial surfactants. *Journal of Applied Microbiology*, 120(4), 868–876. <https://doi.org/10.1111/jam.13049>
- Dijkajaita, A., Humbert, M. V., Borkowski, E., La Ragione, R. M., & Christodoulides, M. (2021). Establishing an invertebrate *Galleria mellonella* greater wax moth larval model of *Neisseria gonorrhoeae* infection. *Virulence*, 12(1), 1900–1920. <https://doi.org/10.1080/21505594.2021.1950269>
- D'Orazio, G., Munizza, L., Zampolli, J., Forcella, M., Zoia, L., Fusi, P., Di Gennaro, P., & La Ferla, B. (2017). Cellulose nanocrystals are effective in inhibiting host cell bacterial adhesion. *Journal of Materials Chemistry B*, 5(34), 7018–7020. <https://doi.org/10.1039/C7TB01923H>
- Falcone, M., De Angelis, B., Pea, F., Scalise, A., Stefani, S., Tasinato, R., Zanetti, O., & Dalla Paola, L. (2021). Challenges in the management of chronic wound infections. *Journal of Global Antimicrobial Resistance*, 26, 140–147. <https://doi.org/10.1016/j.jgar.2021.05.010>
- ISO 10993-5:2009. (2009). *Biological evaluation of medical devices - part 5: Tests for in vitro cytotoxicity*. *International Organization for Standardization*.
- Kennewell, T., Mashtoub, S., Howarth, G., Cowin, A., & Kopecki, Z. (2019). Antimicrobial and healing-promoting properties of animal and plant oils for the treatment of infected wounds. *Wound Practice and Research*, 27(4). <https://doi.org/10.33235/wpr.27.4.175-183>
- Klemm, D., Heublein, B., Fink, H.-P., & Bohn, A. (2005). Cellulose: Fascinating biopolymer and sustainable raw material. *Angewandte Chemie International Edition*, 44(22), 3358–3393. <https://doi.org/10.1002/anie.200460587>
- Klemm, D., Schumann, D., Udhardt, U., & Marsch, S. (2001). Bacterial synthesized cellulose—Artificial blood vessels for microsurgery. *Progress in Polymer Science*, 26(9), 1561–1603. [https://doi.org/10.1016/S0079-6700\(01\)00021-1](https://doi.org/10.1016/S0079-6700(01)00021-1)
- Lahiri, D., Nag, M., Dutta, B., Mukherjee, I., Ghosh, S., Dey, A., Banerjee, R., & Ray, R. R. (2021). Catechin as the most efficient bioactive compound from *azadirachta indica* with antibiofilm and anti-quorum sensing activities against dental biofilm: an in vitro and in silico study. *Applied Biochemistry and Biotechnology*, 193(6), 1617–1630. <https://doi.org/10.1007/s12010-021-03511-1>
- Mannala, G. (2020). *Galleria mellonella* as an alternative in vivo model to study bacterial biofilms on stainless steel and titanium implants. *ALTEX*. <https://doi.org/10.14573/altext.2003211>
- Maslova, E., Osman, S., & McCarthy, R. R. (2023). Using the *Galleria mellonella* burn wound and infection model to identify and characterize potential wound probiotics. *Microbiology*, (6), 169. <https://doi.org/10.1099/mic.0.001350>
- Maslova, E., Shi, Y., Sjöberg, F., Azevedo, H. S., Wareham, D. W., & McCarthy, R. R. (2020). An invertebrate burn wound model that recapitulates the hallmarks of burn trauma and infection seen in mammalian models. *Frontiers in Microbiology*, 11, 998. <https://doi.org/10.3389/fmicb.2020.00998>
- Meftahi, A., Samyn, P., Geravand, S. A., Khajavi, R., Alibakhshi, S., Bechelany, M., & Barhoum, A. (2022). Nanocelluloses as skin biocompatible materials for skincare, cosmetics, and healthcare: Formulations, regulations, and emerging applications. *Carbohydrate Polymers*, 278, Article 118956. <https://doi.org/10.1016/j.carbpol.2021.118956>
- Özdemir, S., Bostanabad, S. Y., Parmaksız, A., & Canatan, H. C. (2023). Combination of St. John's wort oil and neem oil in pharmaceuticals: An effective treatment option for pressure ulcers in intensive care units. *Medicina*, 59(3), 467. <https://doi.org/10.3390/medicina59030467>
- Padmanabhan, S. K., Lionetto, F., Nisi, R., Stoppa, M., & Licciulli, A. (2022). Sustainable production of stiff and crystalline bacterial cellulose from orange peel extract. *Sustainability*, 14(4), 2247. <https://doi.org/10.3390/su14042247>
- Pal, S., Nisi, R., Stoppa, M., & Licciulli, A. (2017). Silver-functionalized bacterial cellulose as antibacterial membrane for wound-healing applications. *ACS Omega*, 2(7), 3632–3639. <https://doi.org/10.1021/acsomega.7b00442>
- Rajan, A., Robertson, M. J., Carter, H. E., Poole, N. M., Clark, J. R., Green, S. I., Criss, Z. K., Zhao, B., Karandikar, U., Xing, Y., Margalef-Català, M., Jain, N., Wilson, R. L., Bai, F., Hyser, J. M., Petrosino, J., Shroyer, N. F., Blutt, S. E., Coarfa, C., ... Maresso, A. W. (2020). Enteroaggregative *E. coli* adherence to human heparan sulfate proteoglycans drives segment and host specific responses to infection. *PLOS Pathogens*, 16(9), Article e1008851. <https://doi.org/10.1371/journal.ppat.1008851>
- Rajas, O., Quirós, L. M., Ortega, M., Vazquez-Espinosa, E., Merayo-Lloves, J., Vazquez, F., & García, B. (2017). Glycosaminoglycans are involved in bacterial adherence to lung cells. *BMC Infectious Diseases*, 17(1), 319. <https://doi.org/10.1186/s12879-017-2418-5>
- Sarkar, P., Acharyya, S., Banerjee, A., Patra, A., Thankamani, K., Koley, H., & Bag, P. K. (2016). Intracellular, biofilm-inhibitory and membrane-damaging activities of nimbolide isolated from *Azadirachta indica* A. Juss (Meliaceae) against methicillin-resistant *Staphylococcus aureus*. *Journal of Medical Microbiology*, 65(10), 1205–1214. <https://doi.org/10.1099/jmm.0.000343>
- Schilcher, K., & Horswill, A. R. (2020). Staphylococcal biofilm development: Structure, regulation, and treatment strategies. *Microbiology and Molecular Biology Reviews*, 84(3), e00026. <https://doi.org/10.1128/MMBR.00026-19>
- Scorzoni, L., De Lucas, M. P., Mesa-Arango, A. C., Fusco-Almeida, A. M., Lozano, E., Cuenca-Estrella, M., Mendes-Giannini, M. J., & Zaragoza, O. (2013). Antifungal efficacy during candida krusei infection in non-conventional models correlates with the yeast in vitro susceptibility profile. *PLoS ONE*, 8(3), e60047. <https://doi.org/10.1371/journal.pone.0060047>
- Sen, C. K. (2019). Human wounds and its burden: An updated compendium of estimates. *Advances in Wound Care*, 8(2), 39–48. <https://doi.org/10.1089/wound.2019.0946>
- Serra, R., Grande, R., Butrico, L., Rossi, A., Settimo, U. F., Caroleo, B., Amato, B., Gallelli, L., & De Francis, S. (2015). Chronic wound infections: The role of *Pseudomonas aeruginosa* and *Staphylococcus aureus*. *Expert Review of Anti-Infective Therapy*, 13(5), 605–613. <https://doi.org/10.1586/14787210.2015.1023291>
- Shi, Y., Wareham, D. W., Yuan, Y., Deng, X., Mata, A., & Azevedo, H. S. (2021). Polymyxin B-triggered assembly of peptide hydrogels for localized and sustained release of combined antimicrobial therapy. *Advanced Healthcare Materials*, 10(22), Article 2101465. <https://doi.org/10.1002/adhm.202101465>
- Srivastava, N., Khan, P. A., Lal, B., Singh, R., Syed, A., Elgorban, A. M., Verma, M., Mishra, P. K., & O'Donovan, A. (2023). Production enhancement of bacterial cellulase cocktail using potato peels waste feedstock and combination of water hyacinth root and pea pod extract as natural nutrient media: Application in bioconversion of potato peels. *Molecular Biotechnology*. <https://doi.org/10.1007/s12033-023-00789-w>
- Süntar, I., Oyardi, O., Akkol, E. K., & Özçelik, B. (2016). Antimicrobial effect of the extracts from *Hypericum perforatum* against oral bacteria and biofilm formation. *Pharmaceutical Biology*, 54(6), 1065–1070. <https://doi.org/10.3109/13880209.2015.1102948>
- Thi, M. T. T., Wibowo, D., & Rehm, B. H. A. (2020). *Pseudomonas aeruginosa* biofilms. *International Journal of Molecular Sciences*, 21(22), 8671. <https://doi.org/10.3390/ijms21228671>
- Tredici, S. M., Buccolieri, A., Tanini, L., Calcagnile, M., Manno, D., & Alifano, P. (2018). Calcite-forming *Bacillus licheniformis* thriving on underwater speleothems of a hydrothermal cave. *Geomicrobiology Journal*, 35(9), 804–817. <https://doi.org/10.1080/01490451.2018.1476626>
- Vanderwoude, J., Fleming, D., Azimi, S., Trivedi, U., Rumbaugh, K. P., & Diggle, S. P. (2020). The evolution of virulence in *Pseudomonas aeruginosa* during chronic wound infection. In , 287. *Proceedings of the Royal Society B: Biological Sciences*, Article 20202272. <https://doi.org/10.1098/rspb.2020.2272>
- Verderosa, A. D., Totsika, M., & Fairfull-Smith, K. E. (2019). Bacterial biofilm eradication agents: A current review. *Frontiers in Chemistry*, 7, 824. <https://doi.org/10.3389/fchem.2019.00824>
- Winter, G. D. (1962). Formation of the scab and the rate of epithelization of superficial wounds in the skin of the young domestic pig. *Nature*, 193(4812), 293–294. <https://doi.org/10.1038/193293a0>
- Yamada, Y., Yukphan, P., Lan Vu, H. T., Muramatsu, Y., Ochaikul, D., Tanasupawat, S., & Nakagawa, Y. (2012). Description of *Komagataeibacter* gen. Nov., with proposals of new combinations (Acetobacteraceae). *The Journal of General and Applied Microbiology*, 58(5), 397–404. <https://doi.org/10.2323/jgam.58.397>
- Zhang, M., Yang, Y., & Acevedo, N. C. (2020). Effect of oil content and composition on the gelling properties of egg-SPI proteins stabilized emulsion gels. *Food Biophysics*, 15(4), 473–481. <https://doi.org/10.1007/s11483-020-09646-8>